Proceedings of 14th IOE Graduate Conference
Peer Reviewed
Year: 2023 Month: December Volume: 14
ISSN: 2350-8914 (Online), 2350-8906 (Print)

Dynamic Response of Rotor – Turbine Assembly for Undamped Free Vibration

Madhav Kandel [a], Prajwal Raj Shakya [b], Mahesh Chandra Luitel [c], Sujan Dahal [d]

[a, b, d] *Department of Automobile and Mechanical Engineering, Thapathali Campus, IOE, Tribhuvan University, Nepal*
[c] *Department of Mechanical Engineering, Pulchowk Campus, IOE, Tribhuvan University, Nepal*
[a] madhav_5004@tcioe.edu.np, [b] pshakya@tcioe.edu.np, [c] mcluintel@ioe.edu.np, [d] sujand458@ioepc.edu.np

Abstract
This research work was carried out to determine the continuous system's natural frequency by mathematically modeling the Pelton turbine unit with the centrally located rigid rotor on the circular flexible shaft, which was simply supported on both ends by rigid bearings and had a rigid runner at the other end that caused the system to overhang. At first, the equation of motion and associated boundary condition were found using the Hamilton principle, and an analytical solution was obtained from the Equation Of motion(EOM). EOM is solved by the assumed mode method using the polynomial shape function for the first mode. The output natural frequency of the system was obtained with an approximate solution for the continuous shaft and disk (runner-rotor) system using the ANSYS simulation, which showed no appreciable deviation from the analytical solution. For the continuous system model, the front whirl's natural frequency increased along with the shaft's rotational speed, while the backward whirl's natural frequency decreased.

Keywords
Mathematical modeling, Continuous System, Hamilton Principle, Assume Mode, Critical Speed, Natural Frequency

1. Introduction

Pelton turbine units are commonly utilized in hydroelectric power plants for their high efficiency and reliability, requiring careful study of rotor dynamics to optimize their performance. Rotor dynamics studies rotating objects, focusing on forces and vibrations. It aims to predict and manage vibrations, reducing vibration-related failure by analyzing transverse/lateral, longitudinal, and torsional vibrations.

Mechanical systems generate oscillations, which can cause vibrations that can cause system failure and workplace accidents. Excessive vibrations waste energy and produce unwanted noise. Designing carefully reduces unwanted vibrations, while natural frequencies occur naturally without external force.

Resonance in turbines increases failure risk due to buckling and shaft deformation. Vibration analysis focuses on amplitudes and natural frequency. Due to high costs and potential damage, dynamic analysis methodologies are needed. The study of the Pelton turbine unit's vibration evaluated its critical frequency, reducing vibration-related failure. This knowledge maximizes the effectiveness, dependability, and lifespan of hydraulic turbine system components and the overall system, as variations in operating conditions should not bring the runner's speed near the critical frequency.

This work investigates the symmetric rotor-bearing system's lateral and torsional vibrations, coupled with external torque, using a modified transfer matrix approach. Disk and shaft orientations are described by the Euler's angles, and the Timoshenko beam is used to simulate the symmetric rotating shaft. A continuous-system approach is employed, focusing on synchronous and superharmonic whirls for increased accuracy [1]. Dynamic analysis is performed on a Pelton turbine unit to determine its natural frequency, while a mathematical model calculates kinetic and strain energy, using Lagrange equations and the Rayleigh-Ritz method for rotor physics [2].

Pelton's turbine units were modeled using mathematical models, including discrete and continuous systems. The governing equations were developed using the Jeffcot rotor model and Rayleigh's energy method and solved using the Rayleigh-Ritz analytical solution method. The natural frequency of the Pelton turbine unit was determined by calculating the effective mass of a simply supported shaft at the ends of the unit as a discrete single-degree-of-freedom system. The result was close to the natural frequency calculated using a continuous system model for the backward and forward whirl [3]. Rotating Euler-Bernoulli shaft model was used. The system's governing equations are a coupled system of differential equations. Free vibration analysis reveals critical speeds for both backward whirl and forward whirl modes. Forward whirl's critical speed increases with operating speed, while backward whirl's increases with speed. The rate of increase in the ratio of successive critical speeds is higher for a simply supported shaft than for a shaft with both ends fixed [4]. Analysis of free transverse vibration generated by flexible rotor bearings at support ends is used to study the dynamic behavior of shafts with various end conditions. This analysis uses an analytical model based on a solid foundation, flexible bearings, and a rigid disk. Kinetic energies, strain energies, and non-conservative work are derived using the assumed mode method. The system's EOM is obtained by substituting these expressions into Lagrange's equation of motion, determining solutions using natural vibrational frequencies [5].

Research demonstrates a method for analyzing forced and free dynamic responses in Pelton turbine units' shafts. The Hamilton principle is used to model water jet impact and derive bending vibration equations, identifying free and forced reactions [6]. Torsional motion and torsional vibration are common causes of failure in rotating mechanical equipment. The equation of motion for a rigid disk and a uniform shaft is taken into account, revealing resonance when critical speed is less than half the natural frequency [7]. This work examines the stability of a rotor system with a nonlinear spinning shaft and stiff disks near critical speeds. It investigates factors affecting linear frequencies, steady-state response, stability, and bifurcations. The study finds that increasing disk mass moment reduces the hardening effect and amplitude of inertia [8]. The Musznyska model and short bearing model are used to model a two-span rotor system, describing nonlinear seal force and oil-film force. Numerical solutions are computed using the fourth-order Runge-Kutta technique. The model examines the dynamic behavior of bearing and disk centers in the horizontal direction [9].

Only one rotating component is considered: the runner disk for the simply supported and overhung condition. However, there is a generator present in the actual device, and it has a revolving component called a rotor. Therefore, the study problem of a turbine rotor that is simply supported and a runner disk that is overhung is taken into consideration.

2. Mathmatical Modeling

Most engineering issues can be solved by mathematically simulating a physical system. For a thorough knowledge of the many traits of the physical systems in real life, mathematical models serve as the governing equations. Here, the rigid rotor with rigid bearing support at positions with the flexible shaft and the overhung rigid runner-bucket assembly (disk) on a continuous shaft were the basic components taken into consideration for the model creation. The figure shows an asymmetrical rotating shaft with an arbitrary cross-section and an undeformed length L. It revolves along its longitudinal primary axis Y at a constant rotational speed. The global coordinate X Y Z and the local coordinate x y z are used to analyze the system's dynamics. The transverse direction of the shaft on the horizontal plane is traveled by x, the longitudinal direction of the shaft is traveled by y, and the transverse direction of the shaft is traveled by z on the vertical plane. The figure represents a portion of the shaft, with deflections along the X, Y, and Z axes designated by u(y, t), v(y, t), and w(y, t), respectively. The shaft is slender and the gravity effect is neglected. Only the transverse vibration of the system is analyzed w(y, t), while the longitudinal and torsional effects are ignored.

2.1 Development of rotational matrix for 312 Euler angle

Any rotation may be expressed in terms of three subsequent rotations about linearly independent axes, which are known as Euler angles. Euler's angles may be used to explain the locations, angular velocities, and angular accelerations of

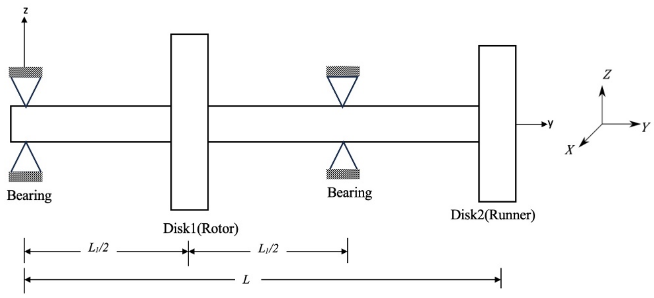

Figure 1: Runner and Rotor Assembly

rotating bodies such as gyroscopes and rotating bodies about their centers of mass (aircraft, turbine shafts, etc.).

To obtain the desired orientation, the disk is first rotated about the Z axis from the initial axis XYZ system to X_1, Y_1, Z_1. The axis Z remains coincident with the z_1 axis. Then by an angle (about the new axis X1–axis to x_2, y_2, z_2. The axis x_2 coincides with the x_1 axis. And finally, by an angle about a new axis y_2 axis. The axis y_2 coincides with y_3 axis. The final coordinates after rotation i.e., X_3, Y_3, Z_3 is denoted by x, y, z.

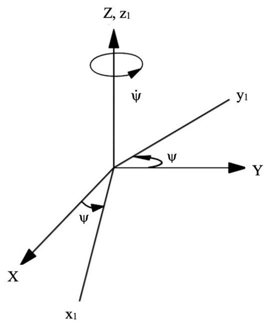

(a) Rotation about Z-axis

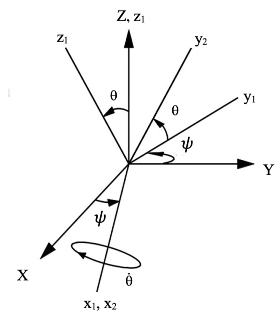

(b) Rotation about x1-axis

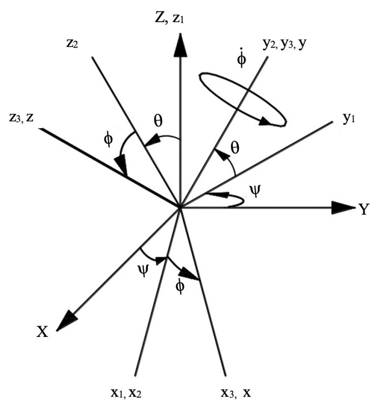

(c) Rotation about y2-axis (spin)

Figure 2: Rotation angles for disks and shaft

$$\begin{bmatrix} x \\ y \\ z \end{bmatrix} = \begin{bmatrix} C\theta C\psi - S\theta S\phi S\psi & C\phi S\psi + S\phi S\theta C\psi & -S\phi C\theta \\ -C\theta S\psi & C\theta & S\theta \\ S\phi C\psi + S\theta C\phi S\psi & S\phi S\psi - S\theta S\phi C\psi & C\phi C\theta \end{bmatrix} \begin{bmatrix} X \\ Y \\ Z \end{bmatrix} \tag{1}$$

Equation 1 represents the link between the fixed inertial coordinates X, Y, and Z and the fixed coordinates of the body x,y,z

2.2 Angular velocity of xyz frame

The xyz frame's angular velocity vector in the moment is given by

$$\Omega = \dot{\psi} Z_1 + \dot{\theta} X_1 + \dot{\psi} Y_2 \qquad [10]$$

$$\begin{bmatrix} \omega_x \\ \omega_y \\ \omega_z \end{bmatrix} = \begin{bmatrix} -\dot{\psi} cos\theta sin\phi + \dot{\theta} cos\phi \\ \dot{\phi} + \dot{\psi} sin\theta \\ \dot{\psi} cos\theta cos\phi + \dot{\theta} sin\phi \end{bmatrix} \tag{2}$$

Where, θ, ϕ, ψ are the Euler angles and $\dot{\phi}, \dot{\theta}, \dot{\psi}$ are its first-time derivatives called the rate of spin, rate of precession, and rate of nutation respectively. For the system considered, the spinning axis is the Y axis and angular motion about X and Z axes are the comparatively small constant rate of spin of shaft $\dot{\phi} = \Omega$ Thus, $cos\theta \approx 1, sin\theta \approx \theta, cos\psi \approx 1$ and $sin\psi \approx \psi$ [11] then the angular velocities becomes

$$\begin{bmatrix} \omega_x \\ \omega_y \\ \omega_z \end{bmatrix} = \begin{bmatrix} -\dot{\psi} sin\phi + \dot{\theta} cos\phi \\ \Omega + \theta \\ \dot{\psi} cos\phi + \dot{\theta} sin\phi \end{bmatrix} \tag{3}$$

2.3 Disk

The disk is assumed to be stiff. Because no strain energy can be determined, the only energy that characterizes this component is kinetic energy.

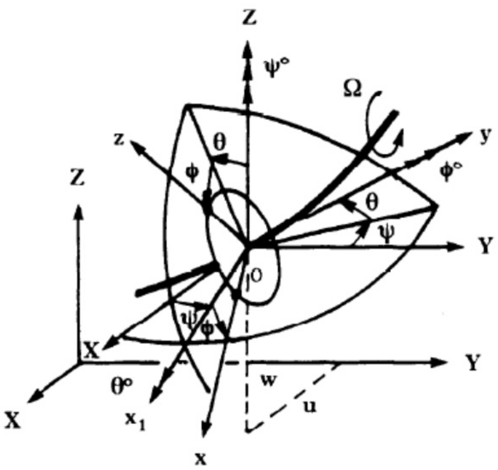

Figure 3: The disk and its reference frames [11]

$$T_{d1} = \left[\frac{1}{2} M_1 \left(\frac{\partial u}{\partial t}\right)^2\right]\Bigg|_{\left(y=\frac{L_1}{2}\right)} + \left[\frac{1}{2} M_1 \left(\frac{\partial w}{\partial t}\right)^2\right]\Bigg|_{\left(y=\frac{L_1}{2}\right)} + \left[\frac{1}{2} I_{xxd1} (\omega_x)^2\right]\Bigg|_{\left(y=\frac{L_1}{2}\right)} + \left[\frac{1}{2} I_{yyd1} (\omega_y)^2\right]\Bigg|_{\left(y=\frac{L_1}{2}\right)} + \left[\frac{1}{2} I_{zzd1} (\omega_z)^2\right]\Bigg|_{\left(y=\frac{L_1}{2}\right)} \tag{4}$$

$$T_{d1} = \left[\frac{1}{2} M_1 (\dot{u}^2 + \dot{w}^2)\right]\Bigg|_{\left(y=\frac{L_1}{2}\right)} + \left[\frac{1}{2} I_{zzd1} \left(\dot{\psi}^2 + \dot{\theta}^2\right)\right]\Bigg|_{\left(y=\frac{L_1}{2}\right)} + \left[\frac{1}{2} I_{yyd1} (\Omega^2 + 2\Omega\dot{\psi}\theta)\right]\Bigg|_{\left(y=\frac{L_1}{2}\right)} \tag{5}$$

$$T_{d2} = \left[\frac{1}{2} M_2 (\dot{u}^2 + \dot{w}^2)\right]\Bigg|_{(y=L)} + \left[\frac{1}{2} I_{zzd2} \left(\dot{\psi}^2 + \dot{\theta}^2\right)\right]\Bigg|_{(y=L)} + \left[\frac{1}{2} I_{yyd2} (\Omega^2 + 2\Omega\dot{\psi}\theta)\right]\Bigg|_{(y=L)} \tag{6}$$

Where, u, w is deflection along transverse axis x and z respectively, M1 and M2 are the mass, and the moment of inertia I_{xxd1}, I_{yyd1}, I_{zzd1} are about the principal axes X, Y, Z axis of the rotor and I_{xxd2}, I_{yyd2}, I_{zzd2} is the moment of inertia of runner. Since disk is thin and assume to be symmetrical, $I_{xx} = I_{zz} = \frac{M_d R_d^2}{4}, I_{yy} = \frac{M_d R_d^2}{2}$

2.4 Shaft

Cross- section of the shaft is shown with the two reference frames one with the inertial XZ with displacement u,v and a rotating frame with the xz with displacement u^*, w^* respectively. Since we are assuming transverse deflection in Z and Xaxis only, we consider only w, u. The shaft has kinetic and strain energy as it is treated as a flexible beam with a uniform circular cross-section.

$$T_S = \frac{1}{2}\rho_S A_S \int_0^L (\frac{\partial u}{\partial t})^2 dy + \frac{1}{2}\rho_S A_S \int_0^L (\frac{\partial w}{\partial t})^2 dy + \frac{1}{2}\rho_S I_{Sxx} \int_0^L (\omega_x)^2 dy + \frac{1}{2}\rho_S I_{Syy} \int_0^L (\omega_y)^2 dy + \frac{1}{2}\rho_S I_{Szz} \int_0^L (\omega_z)^2 dy \tag{7}$$

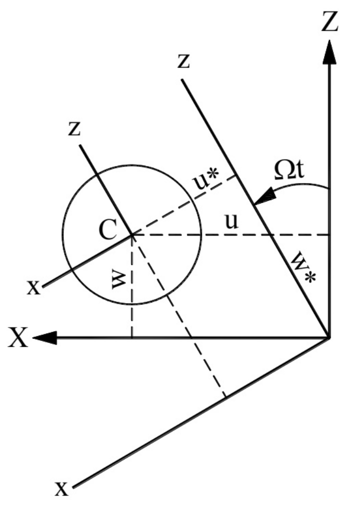

Figure 4: The cross-section of the shaft-source[11]

$$T_S = \frac{1}{2}\rho_S A_S \int_0^L \left(\dot{u}^2 + \dot{w}^2\right) dy + \frac{1}{2}\rho_S I_{Szz} \int_0^L \left(\dot{\psi}^2 + \dot{\theta}^2\right) dy + \rho_S I_{Szz}\Omega^2 L + \rho_S I_{Syy}\Omega \int_0^L (\dot{\psi}\theta) dy \tag{8}$$

ρ_S denotes mass per unit volume, A_S is meant to remain constant and is the cross-sectional area of the shaft., and $I_{sxx} = I_{szz}$ is the cross-sectional area moment of inertia of the shaft around its neutral axis which is equal to $\frac{\pi D^4}{64}$ and $I_{Syy} = \frac{\pi D^4}{32} = 2 * I_{Szz}$, where D is the diameter of shaft.

The shaft's potential energy is determined by

$$V_s = \frac{1}{2} EI_{SZZ} \int_0^L \left[\left(\frac{\partial^2 u}{\partial X^2}\right)^2 + \left(\frac{\partial^2 w}{\partial X^2}\right)^2 \right] dy \tag{9}$$

$$V_s = \frac{1}{2} EI_{Szz} \int_0^L \left[u''^2 + w''^2 \right] dy \tag{10}$$

Where E and I_{Szz} are the Young's Modulus of Elasticity and area moment of inertial of the shaft cross-section about its neutral axis respectively, which is equal to $\frac{\pi D^4}{64}$ $\dot{u}$, $\dot{w}$ denotes the time derivative of u, w and u", w" denotes the double derivative of w with respect to y.

$$\begin{aligned} \theta &= \frac{\partial w}{\partial y}, \dot{\theta} = \frac{\partial \dot{w}}{\partial y} = \dot{w}\prime \\ \psi &= -\frac{\partial u}{\partial y}, \dot{\psi} = -\frac{\partial \dot{u}}{\partial y} = -\dot{u}\prime \\ \phi &= \Omega t, \dot{\phi} = \Omega \end{aligned} \tag{11}$$

Thus, the system's overall kinetic energy may be written as

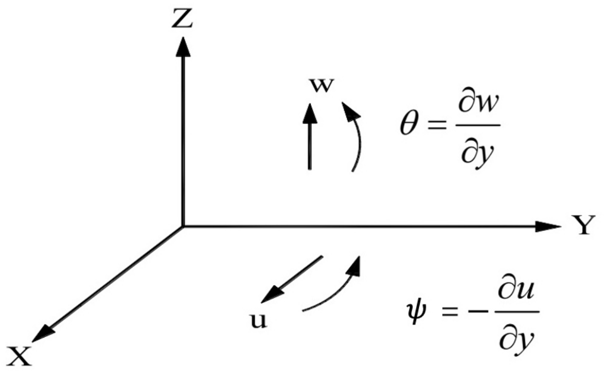

Figure 5: Relation between angular and transverse displacements

$$T = T_{d1} + T_{d2} + T_S$$

$$\begin{aligned} T = {} & \left[\frac{1}{2} M_1 (\dot{u}^2 + \dot{w}^2)\right]\Big|_{\left(y=\frac{L_1}{2}\right)} + \left[\frac{1}{2} I_{zzd1}\left(\dot{\psi}^2 + \dot{\theta}^2\right)\right]\Big|_{\left(y=\frac{L_1}{2}\right)} \\ & + \left[\frac{1}{2} I_{yyd1}(\Omega^2 + 2\Omega\dot{\psi}\,\theta)\right]\Big|_{\left(y=\frac{L_1}{2}\right)} + \left[\frac{1}{2} M_2 (\dot{u}^2 + \dot{w}^2)\right]\Big|_{(y=L)} \\ & + \left[\frac{1}{2} I_{zzd2}\left(\dot{\psi}^2 + \dot{\theta}^2\right)\right]\Big|_{(y=L)} + \left[\frac{1}{2} I_{yyd2}\left(\Omega^2 + 2\Omega\dot{\psi}\theta\right)\right]\Big|_{(y=L)} \\ & + \frac{1}{2}\rho_S A_S \int_0^L (\dot{u}^2 + \dot{w}^2) dy + \frac{1}{2}\rho_S I_{Szz} \int_0^L \left(\dot{\psi}^2 + \dot{\theta}^2\right) dy \\ & + \rho_S I_{Szz}\Omega^2 L + \rho_S I_{Syy}\Omega \int_0^L \left(\dot{\psi}\theta\right) dy \end{aligned} \tag{12}$$

The total Potential energy of the system is expressed as

$$V = V_s = \frac{1}{2} EI_{Szz} \int_0^L \left[u''^2 + w''^2 \right] dy \tag{13}$$

Lagrangian functional for the system can be determined as

$$L = T - V \tag{14}$$

Now applying extended Hamilton's principle

$$\delta \int_{t_1}^{t_2} (L + W_{nc})\, dt = 0 \tag{15}$$

Since we are analyzing free vibration. So, non-conservative force is not considered, and applying the variational principle we get the equation of motion.

2.5 Equation Of Motion and Boundary Condition

The equation of motion for the transverse vibration in x and z direction is given by

$$\begin{aligned} & [-M_1\delta_d\left(y - \frac{L_1}{2}\right)\ddot{u} + I_{zzd1}\delta_d\left(y - \frac{L_1}{2}\right)\ddot{u}'' + I_{yyd1}\Omega\delta_d \\ & \left(y - \frac{L_1}{2}\right)\dot{w}'' - M_2\delta_d(y-L)\ddot{u} + I_{zzd2}\delta_d(y-L)\ddot{u}'' + I_{yyd2}\Omega \\ & \delta_d(y-L)\dot{w}'' - \rho_S A_S\ddot{u} + \rho_S I_{Szz}\ddot{u}'' + \rho_S I_{Syy}\Omega\dot{w}'' - EI_{Szz}u'^{v}] = 0 \end{aligned} \tag{16}$$

$$\begin{aligned} & [-M_1\delta_d\left(y - \frac{L_1}{2}\right)\ddot{w} + I_{zzd1}\delta_d\left(y - \frac{L_1}{2}\right)\ddot{w}'' - I_{yyd1}\Omega\delta_d \\ & \left(y - \frac{L_1}{2}\right)\dot{u}'' - M_2\delta_d(y-L)\ddot{w} + I_{zzd2}\delta_d(y-L)\ddot{w}'' - I_{yyd2}\Omega \\ & \delta_d(y-L)\dot{u}'' - \rho_S A_S\ddot{u} + \rho_S I_{Szz}\ddot{w}'' - \rho_S I_{Syy}\Omega\dot{w}'' - EI_{Szz}w'^{v}] = 0 \end{aligned} \tag{17}$$

Boundary conditions associated with the shaft for the assumed system are

$$\left[EI_{Szz}u''\delta u\prime\right]\big|_0^L \tag{18}$$

$$\left[EI_{Szz}w\prime\prime\delta w\prime\right]\big|_0^L \tag{19}$$

$$[-I_{zzd1}\delta_d\left(y-\frac{L_1}{2}\right)\ddot{u}'\delta u-I_{yyd1}\Omega\delta_d\left(y-\frac{L_1}{2}\right)\dot{w}'\delta u-I_{zzd2}\delta_d(y-L)\ddot{u}'\delta u-I_{yyd2}\Omega\delta_d(y-L)\dot{w}'\delta u-\rho_S I_{Szz}\ddot{u}'\delta u-\rho_S I_{Syy}\Omega\dot{w}'\delta u+EI_{Szz}u'''\delta u]|_{y=0}^{y=L}=0 \quad (20)$$

$$[-I_{zzd1}\delta_d\left(y-\frac{L_1}{2}\right)\ddot{u}'\delta u-I_{yyd1}\Omega\delta_d\left(y-\frac{L_1}{2}\right)\dot{w}'\delta u-I_{zzd2}\delta_d(y-L)\ddot{u}'\delta u-I_{yyd2}\Omega\delta_d(y-L)\dot{w}'\delta u-\rho_S I_{Szz}\ddot{u}'\delta u-\rho_S I_{Syy}\Omega\dot{w}'\delta u+EI_{Szz}u'''\delta u]|_{y=0}^{y=L}=0 \quad (21)$$

The Rayleigh-Ritz technique is often referred to as the assumed modes method. To properly describe the rotor's lateral vibration behavior, the displacements variable u, w must be written in terms of the shape function $\beta(y)$ before using the formulas obtained from the extended Hamilton equation.

$$\begin{aligned} u(y,t)&=\{\beta(y)\}^T\{U(t)\}=\beta U\\ w(y,t)&=\{\beta(y)\}^T\{W(t)\}=\beta W \end{aligned} \quad (22)$$

Where $\beta(y)^T$ is the orthogonal shape function that should satisfy the above boundary condition from equation 4.18 to 4.21. Substituting equation 4.22 in the equation of motion in equations 4.16 and 4.17 and applying the orthogonality principle, we get the ordinary differential equation of motion for i^{th} mode for $U_i(t)$ and $W_i(t)$ can be obtained as

$$M_i\ddot{U}_i+C_i\dot{W}_i+K_iU_i=0 \quad (23)$$

$$M_i\ddot{W}_i-C_i\dot{U}_i+K_iW_i=03 \quad (24)$$

$$\begin{aligned} (\lambda_i)_1&=\left[\frac{1}{2}\left[-\left\{\left\{\frac{C_i}{M_i}\right\}^2+\frac{2K_i}{M_i}\right\}-\sqrt{\left\{\frac{C_i}{M_i}\right\}^4+4\left\{\frac{C_i}{M_i}\right\}^2\times\frac{K_i}{M_i}}\right]\right]^{\frac{1}{2}}\\ (\lambda_i)_2&=\left[\frac{1}{2}\left[-\left\{\left\{\frac{C_i}{M_i}\right\}^2+\frac{2K_i}{M_i}\right\}+\sqrt{\left\{\frac{C_i}{M_i}\right\}^4+4\left\{\frac{C_i}{M_i}\right\}^2\times\frac{K_i}{M_i}}\right]\right]^{\frac{1}{2}} \end{aligned} \quad (25)$$

Where M_i is the modal mass, C_i is the modal damping, and K_i is the modal stiffness which is given

$$\begin{aligned} M_i=\Bigg[&-\int_0^L M_1\,\delta_d\left(y-\frac{L_1}{2}\right)\beta_\mathrm{i}(\mathrm{y})\beta_\mathrm{i}(\mathrm{y})dy+\int_0^L I_{zzd1}\delta_d\left(y-\frac{L_1}{2}\right)\beta_\mathrm{i}''(\mathrm{y})\beta_\mathrm{i}''(\mathrm{y})dy-\int_0^L M_2\delta_d(y-L)\beta_\mathrm{i}(\mathrm{y})\beta_\mathrm{i}(\mathrm{y})dy\\ &+\int_0^L I_{zzd2}\delta_d(y-L)\beta_\mathrm{i}''(\mathrm{y})\beta_\mathrm{i}''(\mathrm{y})dy-\int_0^L\rho_S A_S\beta_\mathrm{i}(\mathrm{y})\beta_\mathrm{i}(\mathrm{y})dy+\int_0^L\rho_S I_{Szz}\beta_\mathrm{i}''(\mathrm{y})\beta_\mathrm{i}''(\mathrm{y})dy\Bigg] \end{aligned} \quad (26)$$

$$\begin{aligned} C_i=\Bigg[&\int_0^L I_{yyd1}\,\Omega\delta_d\left(y-\frac{L_1}{2}\right)\beta_\mathrm{i}''(\mathrm{y})\beta_\mathrm{i}''(y)dy\\ &+\int_0^L I_{yyd2}\Omega\delta_d(y-L)\beta_\mathrm{i}''(\mathrm{y})\beta_\mathrm{i}''(y)Wdy\\ &+\int_0^L\rho_S I_{Syy}\Omega\beta_\mathrm{i}''(\mathrm{y})\beta_\mathrm{i}''(y)dy\Bigg] \end{aligned} \quad (27)$$

$$K_i=\left[-\int_0^L EI_{Szz}\beta_\mathrm{i}^{\mathrm{iv}}(\mathrm{y})\beta_\mathrm{i}^{\mathrm{iv}}(\mathrm{y})dy\right] \quad (28)$$

2.6 Development of Polynomial Shape Functions

Since the highest power in the equation of motion is four so polynomial shape function can be assumed to have an order of four or higher. Hence, the first modes mode shape can be assumed as

$$\beta_1=y^5+A_4y^4+A_3y^3+A_2y^2+A_1y+A_0 \quad (29)$$

A_i, B_i are the coefficients that can be determined by using the boundary conditions and orthogonal relationships of the mode shape function. Using the Boundary Conditions

$$\begin{aligned} &\beta_i(0)=0,\ \beta_i''(0)=0,\ at\ y=0\\ &\beta_i''(L)=0,\ \beta_i'''(0)=0,\ at\ y=L\\ &\beta_i(L_1)=0,\ ,\ at\ y=L_1 \end{aligned} \quad (30)$$

The coefficients of polynomial mode shape functions are determined as

$$\begin{aligned} &A_O=0,\ A_1=\frac{40}{12}LL_1^3-20L^2L_1^2-L_1^4,\ \ A_2=0,\\ &A_3=\frac{20}{6}L^2,\ A_4=-\frac{40}{12}L \end{aligned} \quad (31)$$

Substituting these coefficients into Equations 29 the expressions for the first mode shape function for a system are established as:

$$\begin{aligned} \beta_1=&y^5+\left(-\frac{40}{12}L\right)y^4+\left(\frac{20}{6}L^2\right)y^3+\\ &\left(\frac{40}{12}LL_1^3-20L^2L_1^2-L_1^4\right)y \end{aligned} \quad (32)$$

3. Results and Discussion

3.1 Numerical Results

The first mode of a shaft disk system is solved numerically as an example, as shown in figure 6. The parameters of the hydropower unit that is used for analysis are shown in Table 1.

Analytical solutions were found for mathematical models to determine natural frequencies under undamped free vibration conditions, and their outcomes were analyzed using various models Using Eqs (1), (2) and (3), equivalent mass (Mi), equivalent damping coefficient (Ci) and stiffness (Ki) for the first mode is found to be

$Mi=-4.45\times10^9\,kg$

$Ci=2.713\times10^9\times\Omega$

$Ki=-7.805\times10^{13}$

Table 1: Model Parameters

SN	Parameters	Values
1	Mass of disk1, M_1	35000 kg
2	Diameter of disk1, D_1	240 cm
3	Moment of inertia disk1 along xx,zz axis, I_{zzd1}	12600 kgm^2
4	Polar Moment of inertia of disk1 along yy axis, I_{yyd1}	25200 kgm^2
5	Mass of disk1, M_2	2575 kg
6	Diameter of disk1 D_2	176 cm
7	Moment of inertia disk2 along xx,zz axis, I_{zzd2}	499 kgm^2
8	Polar Moment of inertia of disk2 along yy axis, I_{yyd2}	998 kgm^2
9	Density of Shaft, ρ_s	7850 Kg/m^3
10	Diameter of Shaft, D_s	50 cm
11	Youngs Modulus of Elasticity of the Shaft Material, E	202Gpa
12	Distance between the support L_1	3000 mm
13	Total length of the shaft, L	4300 mm
14	Shaft cross-sectional area moment of inertia about its transverse axis	0.003067 m^4
15	Shaft cross-sectional Polar Area moment of inertia about its longitudinal axis	0.006135m^4
16	Cross section area of shaft	0.1963 m^2

Table 2: Analytical Results

Modes	ω rad/s	Frequency Hz	Critical Speed rpm
First Mode FW	212.268	33.784	2027.069
First Mode BW	104.519	16.633	998.026

3.2 Results from Simulation

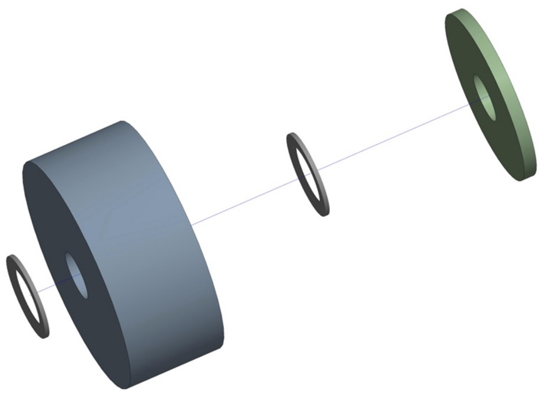

Figure 6: Ansys Simulation Setup

Table 3: Simulation Results

Modes	Frequency Hz	Critical Speed rpm	Error
First mode FW	33.527	210.66	0.763%
First mode BW	17.1059	107.48	2.3%

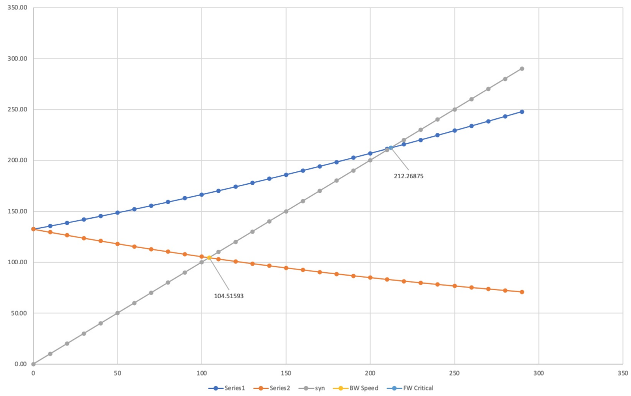

Figure 7: Campbell Diagram from analytical solution

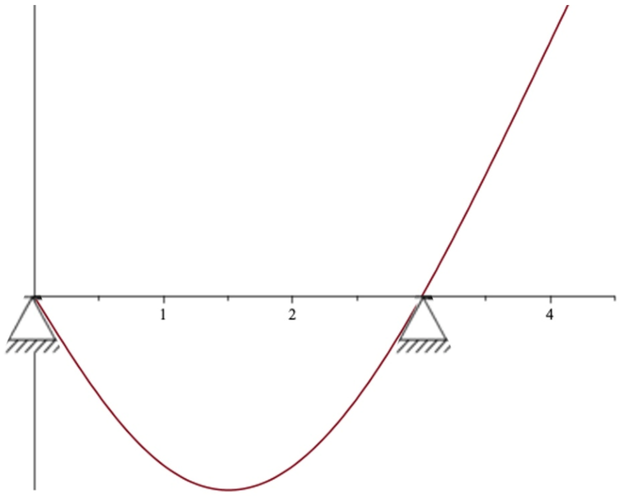

Figure 8: First mode shape from the analytical solution

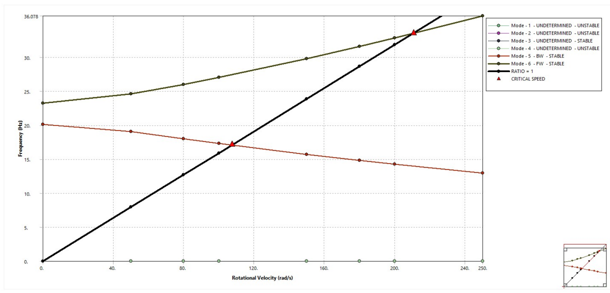

Figure 9: Campbell Diagram from ANSYS simulation

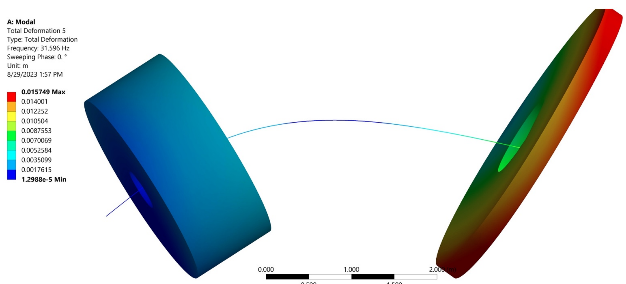

Figure 10: First mode FW shape from ANSYS simulation

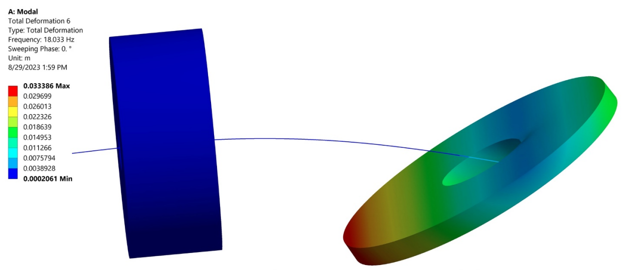

Figure 11: First mode BW shape from ANSYS simulation

4. Conclusion

The real Pelton turbine unit's mathematical models were created as continuous system models. The governing equations for continuous system models were derived by computing the kinetic and strain energy of the shaft and disk. Natural frequencies were found using the Rayleigh-Ritz analytical solution technique to the equations of motion obtained by applying the Hamilton principle and Lagrange's equation. Analytically, the natural frequencies and critical speed were found to be 104.519 rad/sec for the backward whirl and 212.268 rad/sec for the forward whirl. From the ANSYS simulation, the natural frequencies and critical speed were found to be 210.66 rad/sec for backward and 107.48 rad/sec forward whirl. The output natural frequency of the system was obtained with an approximate solution for the continuous shaft and disk (runner-rotor) system using the ANSYS simulation, which showed no appreciable deviation from the analytical solution with the error of 0.763% and 2.3% for the Forward whirl and Backward Whril respectively. Natural frequency and critical speed calculated from this study can be used to study reliability of hydropower.

Acknowledgments

The author(s) is/are grateful to Professor Dr.Mahesh Chandra Luitel, Department of Mechanical Engineering, Pulchowk Campus, Assistant Professor Er. Subodh Kumar Ghimire, Department of Mechanical and Automobile Engineering, Thapathali Campus, and Assistant Professor Er. Sushant Raj Giri, Department of Industrial Engineering, Thapathali Campus for their continuous technical support and suggestions for conducting this research work and also to Assistant Professor Sanjeev Karki, Advance College of Management for his support and suggestions.

References

[1] Sheng-Chung Hsieh, Juhn-Horng Chen, and An-Chen Lee. A modified transfer matrix method for the coupling lateral and torsional vibrations of symmetric rotor-bearing systems. *Journal of Sound and Vibration*, 289:294–333, 01 2006.

[2] Aman Rajak, Prateek Shrestha, Manoj Rijal, Bishal Pudasaini, and Mahesh Chandra Luintel. Dynamic analysis of pelton turbine and assembly. In *Proceedings of IOE Graduate Conference*, pages 103–109, 2014.

[3] Laxman Motra and Mahesh Chandra Luintel. Free vibration analysis of selected pelton turbine using dynamic approach. In *Proceedings of IOE Graduate Conference*, volume 5, pages 229–236, 2017.

[4] Mahesh Chandra Luintel. Dynamic response of continuous shafts with different end conditions. *Journal of Innovations in Engineering Education| Vol*, 2(1), 2019.

[5] Janak Kumar Tharu, Nishant Bhatta, Sanjeev Karki, and Mahesh Chandra Luintel. Free vibration analysis of simply supported pelton turbine: A case of flexible rotor bearings. In *Proceedings of IOE Graduate Conference*, 2019.

[6] Mahesh Luintel and Tri Bajracharya. Dynamic response of a timoshenko shaft with a rigid disk. *Journal of Engineering and Applied Sciences*, 14:1239–1246, 01 2019.

[7] Bassem Al-Bdor. Modeling the coupled torsional and lateral vibrations of unbalanced rotors. *Computer Methods in Applied Mechanics and Engineering*, 190:5999–6008, 08 2001.

[8] Majid Shahgholi, Siamak Khadem, and Saeed Bab. Nonlinear vibration analysis of a spinning shaft with multi-disks. *Meccanica*, 50, 03 2015.

[9] Wei Li, De-ren Sheng, Jian-hong Chen, and Yong-qiang Che. Modeling a two-span rotor system based on the hamilton principle and rotor dynamic behavior analysis. *Journal of Zhejiang University-SCIENCE A*, 11(15):883–895, 2014.

[10] T Greenwood Donald. *Principles of Dynamics*. Prentice-Hall, 2003.

[11] Pedro Paulo, Yoann Lage, Miguel Matos Neves, N.M.M. Maia, and F. Lau. A time-domain methodology for rotordynamics: Analysis and force identification. *Civil-Comp Proceedings*, 99, 09 2012.